Theoretical determination of a model molecule for the catalytic upcycling of polyolefins

Jessica Ortega-Ramos,[1] Mikael Maraschin,[2] Gerardine G. Botte[1,], Joseph A. Gauthier[2,]**

1. Institute for Sustainability and Circular Economy, Department of Chemical Engineering, Texas Tech University

2. Department of Chemical Engineering, Texas Tech University, Texas Tech University

AUTHOR INFORMATION

Corresponding Authors

*Gerardine G. Botte –Institute for Sustainability and Circular Economy, Department of Chemical Engineering, Texas Tech University, Lubbock, Texas 79409, United States, Email: gerri.botte@ttu.edu

*Joseph A. Gauthier – Department of Chemical Engineering, Texas Tech University, Lubbock, Texas 79409, United States, Email: Joe.Gauthier@ttu.edu

ABSTRACT. Considering the severe environmental and humanitarian implications of global plastic waste accumulation, understanding polyolefin catalytic degradation is essential. Accordingly, a model compound would improve experiments' reproducibility and simplify theoretical models. Therefore, this study aimed to determine the minimum number of monomers necessary to represent the degradation and upcycling of polyethylene and polypropylene over metal catalysts. Using density functional theory (DFT) calculations, we evaluated how polymer's chain length affects reaction energies and energy barriers for C-H and C-C cleavage over stepped transition metal surfaces. We found that chain length does not significantly affect the C-H and C-C cleavage reaction energies and the C-H cleavage energy barriers. Our findings suggest that ethane may be suitable as a model to study polyethylene's catalytic C-H and C-C cleavage. Although such a simple molecule cannot capture complex transport and entanglement phenomena in full polymers, it remains useful for determining reaction energetics in complex systems.

TOC GRAPHICS

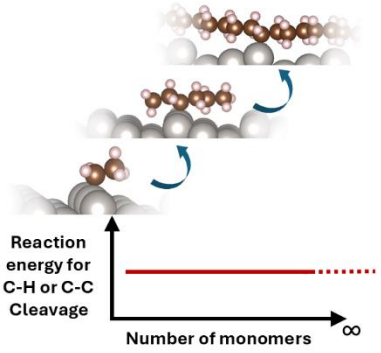

KEYWORDS. DFT, Polyethylene, Chain length effect, Plastic degradation, C-H cleavage, C-C cleavage.

Plastic waste rapidly accumulates in terrestrial and aquatic landscapes, severely threatening human health and the environment. In 2019, only 9% of plastics were recycled globally, while 49% ends up in landfill, 19% was incinerated, and 22% was disposed into uncontrolled dumpsites (possibly leading to accumulation in bodies of water), or burned in open pits.[1,2] A significant component of this plastic waste is polyethylene (PE) and polypropylene (PP), both of which are produced on an enormous scale and are utilized specifically for their exceptional stability over extended timescales.[3] Traditional methods for polyolefin upcycling,[4] like pyrolysis,[5] hydrogenolysis,[6] and solvolysis,[7] are energy-intensive or require toxic/flammable chemicals. Alternatively, new approaches like biodegradation,[8] photocatalysis,[9] and electrocatalysis[10] are performed in relatively mild conditions but typically suffer from low conversion efficiencies, slow kinetics, and as-of-yet unresolved mass transport challenges.[11]

To effectively improve upon new and existing upcycling methods, gaining a molecular-level understanding of the catalytic C-C and C-H bond scission through highly reproducible experimental and theoretical studies is essential. Yet, fundamental research of this kind is challenging due to the size and complexity of the polymer structure, which involves different degrees of crystallinity, branching, molecular weight, and the presence of impurities and additives that can significantly modify its reactivity.[12] A model molecule with similar chemical reactivity would simplify the theoretical analysis and significantly improve the reproducibility of experiments, given the higher availability of pure, well-characterized, low molecular weight compounds. However, to our knowledge, no general criteria exist in the literature to select a compound that accurately represents the same chemistry as the polymer for the heterogenous catalytic activation of the C-H and C-C bond. In published literature reports studying polyethylene,

when simplification was needed, the selection of the chain length was made to fit the necessities of the particular experiment but without clear universal criteria.[13–16]

The number of monomers needed to observe convergence in the kinetics and thermodynamics of C-C bond cleavage in the gas phase was investigated previously. Knyazev[17] demonstrated through molecular dynamic simulations that the per-bond rate constant for thermal C-C bond breaking increases with the chain length from ethane (C2) to decane (C10), but between C10 and C50, there was no significant change in the per-bond rate constant. Also, Alkorta and Elguero[18] calculated the bond dissociation energies (BDE) of C-C bonds in n-alkanes of increasing chain length from ethane to decane at different theory levels: G2MP2, G2, G3MP2B3, G3, and G3B3 within Gaussian-03 package. The authors observed that the BDE of the middle C-C bond stabilizes after ten carbons to a value of -371.8 kJ mol^{-1}, corresponding to the n-alkane of infinite length. Both of these research works focused on gas-phase cleavage of the C-C bond in an isolated molecule. However, critically, the effect of chain length on C-C bond-scission over a catalyst has not been explored. It is essential to evaluate this type of system since heterogeneous catalysis can break down polyolefins at substantially milder conditions and with higher selectivity than the uncatalyzed gas-phase process.

This study aimed to determine the minimum chain length required to accurately represent the degradation and functionalization of polyethylene and polypropylene over a metal catalyst. To achieve this, density functional theory (DFT) calculations were conducted to evaluate the impact of chain length on the reaction energies and energy barriers associated with the C-H and C-C bond cleavage of polyethylene and polypropylene oligomers on Pt(211). These results represent the first step in defining a polyethylene and polypropylene model molecule in heterogenous systems, which

will bring the opportunity to conduct more reproducible experiments and carry out theoretical studies in catalyzed polyolefin upcycling and recycling.

Before analyzing the results, we report the approaches taken to determine the reaction energies and energy barriers in this work, in particular the use of generalized machine learning potentials to find lower energy configurations of the system, the handling of the supercell size effect in the calculations, and the selection of the proper initial state.

A fine-tuned machine learning model was used as a substitute for the DFT relaxation step needed in the minima hopping,[19] accelerating the process of screening hundreds of configurations to search for the one with the lowest energy. The machine learning model was developed by the Open Catalyst Project (OCP), a collaborative research effort between Fundamental AI Research (FAIR) at Meta AI and Carnegie Mellon University's (CMU) Department of Chemical Engineering.[20] The model consists of a Graph Neural Network (GNN), where each graph is represented by a set of vertices (atoms) and edges (interaction between atoms).[21] One of the main tasks of the model is to predict the energy and forces given a structure as an input. Although the dataset for this model includes more than 200 million structures involving metal (OC20)[22] and oxide (OC22)[23] slabs with and without a variety of adsorbates, these small adsorbates (five atoms on average) are considerably different from the long hydrocarbons studied in this work. This difference caused poor accuracy in the prediction of the system's total energy for a dataset created from DFT relaxations of PE and PP oligomers over Pt(211), illustrated by the parity plot of Figure 1 (a) and the relatively large mean absolute error (MAE) of 0.452 eV/atom.

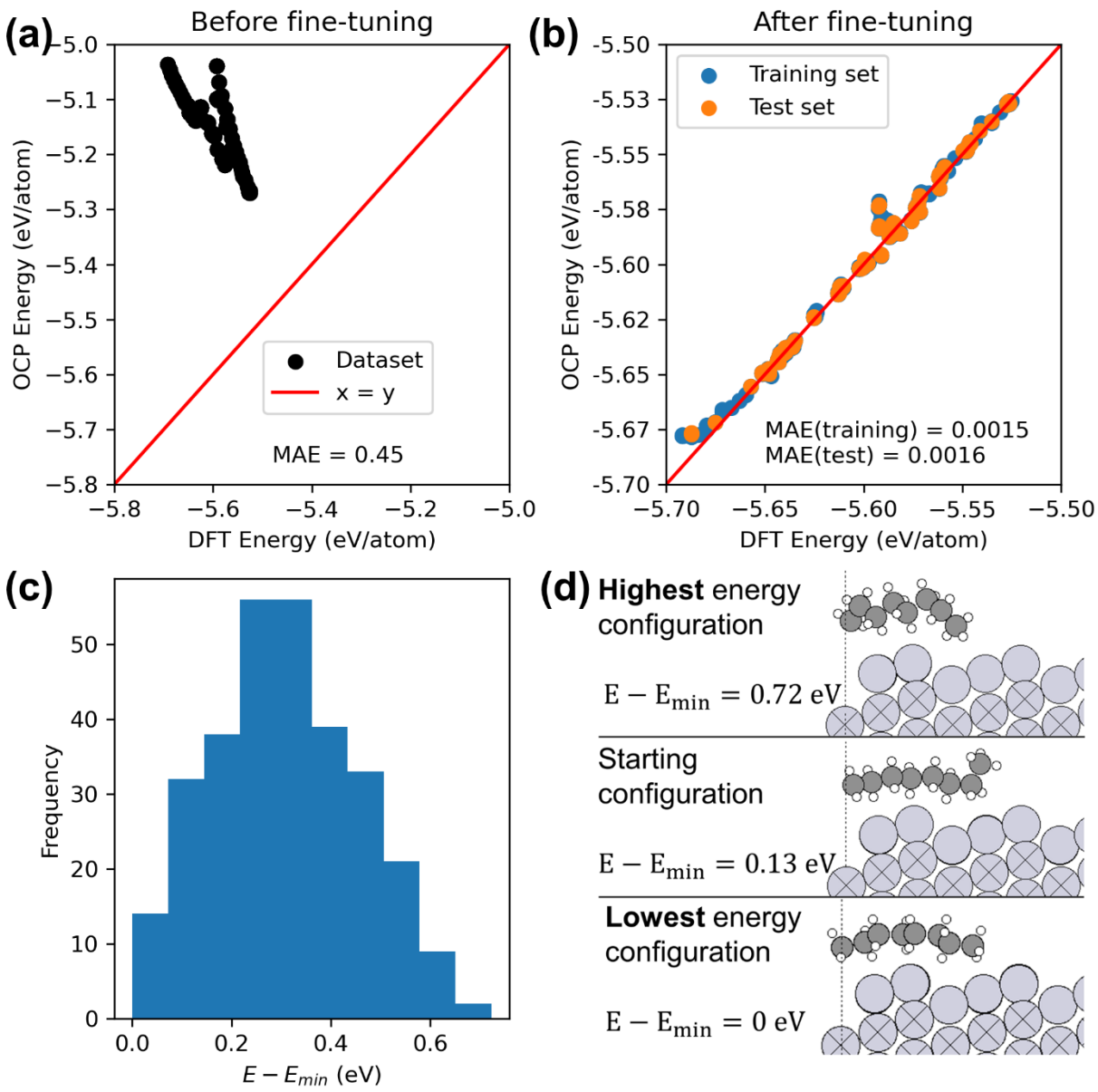

Figure 1. (a) Parity plot showing the correspondence between the DFT energy and the prediction made by the machine learning model using the GemNet-OC OC20+OC22 checkpoint (OCP energy) for the dataset of 2005 images created in this work. The mean absolute error (MAE) is in units of eV/atom. (b) Parity plot showing the correspondence between the DFT and OCP energy (after the fine-tuning) for the training and test datasets. (c) Distribution of the configuration's energies, relative to the lowest energy configuration (Emin), for the system consisting of octane

adsorbed over a platinum slab. (d) Starting configuration, highest and lowest energy configuration of the system (platinum slab + adsorbed octane) found using minima hopping.

As a result, the machine learning model required fine-tuning,[24] described in detail in the Supporting Information. After the fine-tuning, the model's performance improved significantly, demonstrated by the parity plot in Figure 1 (b) and the lower MAE of 0.0015 eV/atom for the training set and 0.0016 eV/atom for the test set. The fine-tuned machine learning model was used in the relaxation and annealing steps of the minima hopping. This approach made it possible to quickly find a lower energy configuration compared to the starting configuration in most cases. For instance, the energy distribution, relative to the minimum energy, for the 300 configurations found for the system of a Pt(211) slab with an adsorbed octane is shown in Figure 1 (c). In this Figure, most of the configurations differ from the minimum energy configuration by 0.3 eV. The difference between the geometry of the lowest and highest energy configurations is illustrated in Figure 1(d), where the starting configuration is also shown for comparison. Here, the main difference between the configurations is the orientation of the octane over the surface, which can cause an energy difference as high as 0.7 eV. It is important to note that minima hopping employed with the fine-tuned machine learning model did not always find a lower energy configuration, and when it did, this configuration is not necessarily guaranteed to be the global minimum of the system.

Once the lower energy configuration was identified using minima hopping, the system was relaxed using DFT. However, it was found that the system's energy depends on the supercell size in a counterintuitive way. This effect is shown in Figure 2 (a), where the system's energy generally increases as the surface area increases. In other words, the system becomes less stable as the

surface coverage decreases, suggesting an attractive adsorbate-adsorbate interaction, unlike those typically found for small molecules on transition metal surfaces. The van der Waals (vdW) interactions are likely not responsible for this trend since it does not change when a vdW correction (Grimme's DFT-D3 method)[25] is omitted from the calculation. This trend might suggest that polypropylene oligomers prefer interacting with themselves rather than with the metal surface.

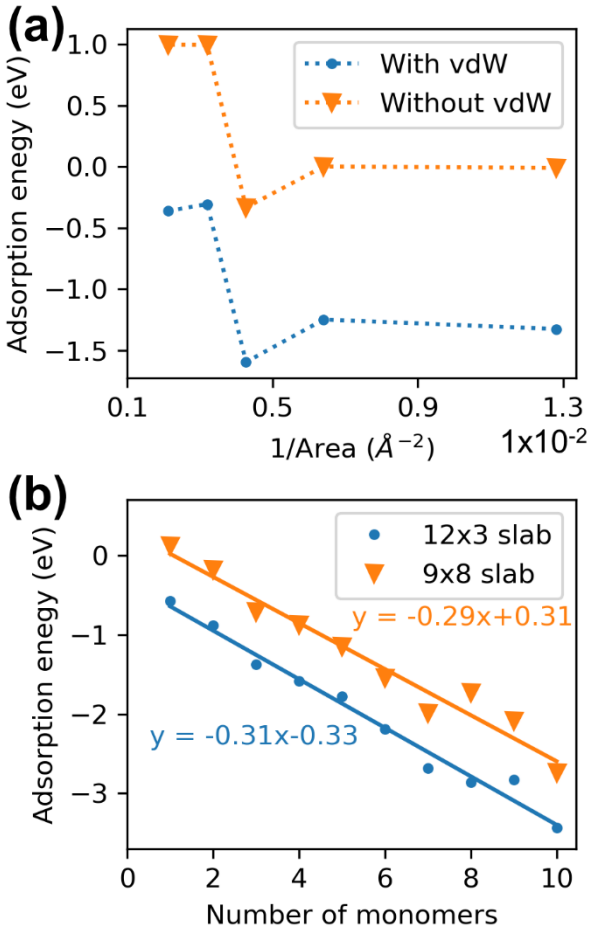

Figure 2. (a) Adsorption energy of polypropylene trimer (three monomers) over Pt(211) as a function of the reciprocal of the surface area of the slab. The surface area was obtained by multiplying the supercell lattice vectors a and b parallel to the XY plane. The metal slabs tested consisted of 3x4, 6x4, 9x4, 6x8, and 9x8 atoms. (b) Adsorption energy as a function of the number of polypropylene monomers for two different metal slab sizes consisting of 12x3 and 9x8 atoms.

Ideally, the calculations should be performed in the limit of infinite supercell size, where this parameter no longer affects the system's energy, as this will enable a fairer comparison as the chain length increases. Still, as Figure 2 (a) demonstrates, the energy converges for a metal slab larger than 6x8 atoms, which would be computationally intractable in this study. To work around this issue, we made all the comparisons between energies at different chain lengths using the same supercell size. The selection of a specific supercell size did not affect the type of trend observed for the chain length. This statement is demonstrated in Figure 2 (b), where the adsorption energy of polypropylene oligomers is shown as a function of the number of monomers for two supercell sizes. This figure illustrates that, despite different energy values (i.e., intercept), the linear *trend* found for the adsorption as a function of the number of monomers was independent of the supercell size.

Aside from the supercell size effect, another important consideration was the selection of the initial state when the final state is the cleaved bond (C-H or C-C) over the metal surface, for which there are two possibilities to consider. In the first case, the initial state combines the gas-phase hydrocarbon and the clean platinum slab. For simplicity, we denote the reaction energies calculated with this initial state as RE1. Although this initial state is well-defined, the RE1s highly depend on the van der Waals attractive interactions between the hydrocarbon and the metal. This dependency is evidenced by the linear decrease in the RE1 as the number of monomers increases, as shown in Figure 3 (a), which follows the same trend as the adsorption energies for n-alkanes over a metal surface reported in the literature[26–28] and calculated in this work.

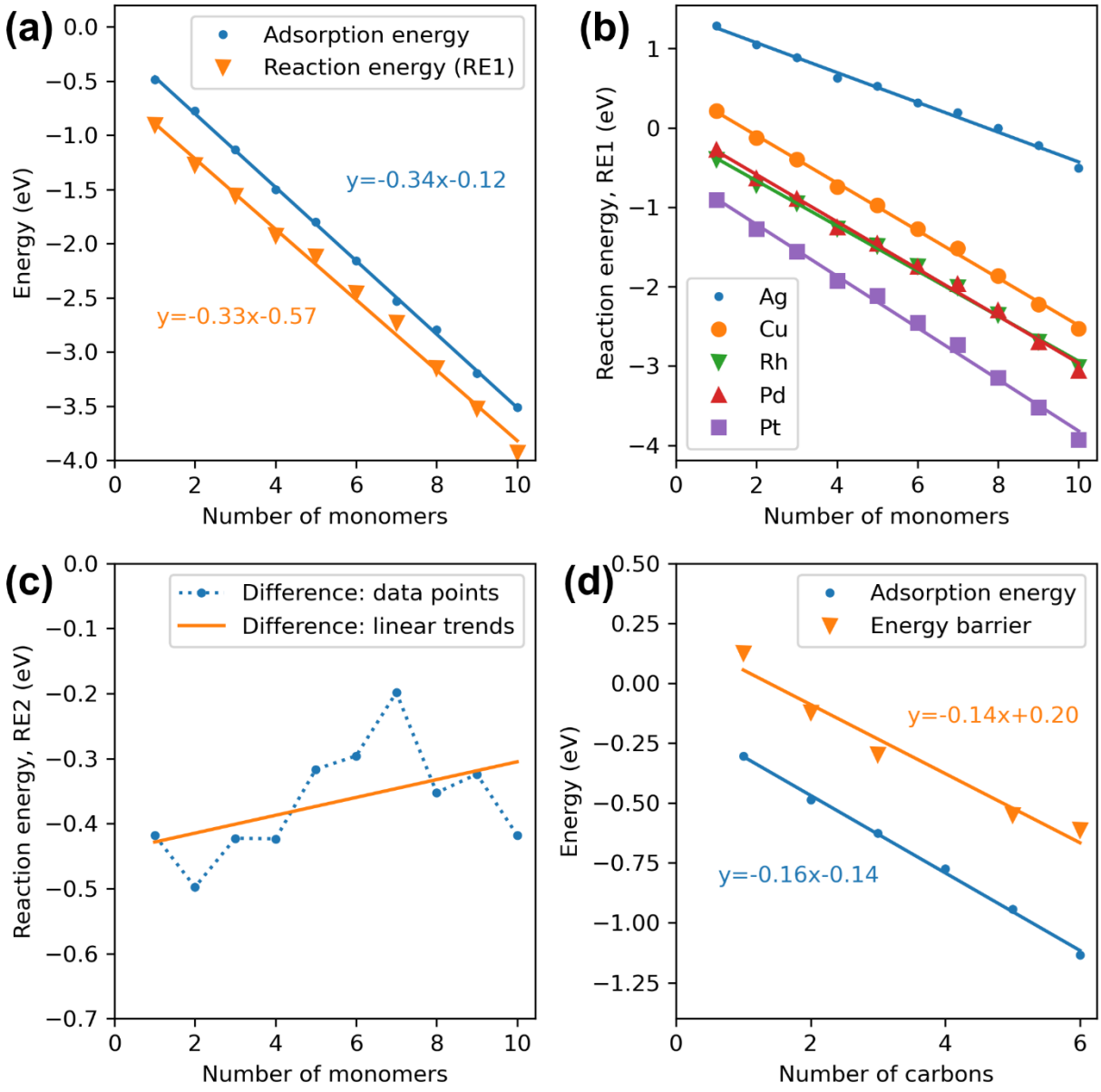

Figure 3. (a) Reaction energies for the C-H cleavage (referred to as RE1 since the initial state is the clean metal slab and gas-phase hydrocarbon) and adsorption energies as a function of the number of monomers in the polyethylene oligomers over Pt(211). One monomer is equivalent to an ethane molecule. (b) RE1 for the C-H cleavage as a function of the number of monomers in the polyethylene oligomers for different metals. (c) Reaction energies for the C-H cleavage (RE2 since the initial state is the adsorbed hydrocarbon) as a function of the number of monomers in the

polyethylene oligomers. The RE2s were calculated in two different ways: by the difference between the data points and by the difference between linear trends. (d) Energy barriers for the C-H cleavage and adsorption energies as a function of the number of carbons in the n-alkane.

We attribute the linear trend to the direct proportionality of the vdW interaction and the surface area of the hydrocarbon; no linear trend is observed when the vdW correction is omitted from the calculation (c.f. Figure S2 in the Supporting Information). The linear behavior of the RE1s is not specific to platinum since it also occurs in other metals, as shown in Figure 3 (b). In all these cases, the RE1s follow the same linear trend as the adsorption energies with a similar slope within a 10% error (c.f. Figures S3 to S6 in the Supporting Information).

In the second case, which we denote as RE2, the initial state is the physically adsorbed hydrocarbon over the platinum surface. This initial state would allow subtraction of the hydrocarbon-metal interaction to see the effect of increasing the number of monomers in the C-H and C-C bond strength. However, the adsorbed hydrocarbon is more difficult to unambiguously define since there are many ways in which the hydrocarbon can adsorb to the metal surface, and the number of possible configurations grows combinatorically as hydrocarbon chain length increases. Thus, finding the most stable absorption configuration (i.e., the global energy minimum of the system) for long hydrocarbon chains becomes challenging, even using minima hopping. The many possibilities for the adsorbed hydrocarbon introduce high dispersion to the RE2s when they are calculated as the difference between the adsorbed hydrocarbon (initial state) and the cleaved bond over the metal (final state) for each chain length (see Figure 3 (c), labeled as "difference: data points"). This result differs from the trend Ding et al.[28] reported, where the RE2s for the C-H cleavage of n-alkanes over Pt(111) and Pt_{55} cluster increased slightly with the number of carbons, from one to six carbons. The discrepancy between these results might be due to the difference in

the range of n-alkanes evaluated. Smaller n-alkanes have fewer possible configurations; thus, the associated energies present lower dispersion. Also, the slight increase in the previously reported RE2s could be considered a small fluctuation due to the differences in adsorption configuration between the n-alkanes.

An alternative approach to determining RE2 is to calculate the difference between the linear trends for the adsorption energy and RE1 found in Figure 3 (a). The result of this calculation, as shown in Figure 3 (c) (labeled as "difference: linear trend"), is that the RE2 slightly increases as the number of monomers increases, but the overall change is essentially negligible. This result is evident from the fact that the slopes for the linear trends of adsorption energies and RE1s are within ~10%. Considering only the thermodynamics, this result implies that the system will release the same energy for the C-H cleavage in adsorbed ethane and adsorbed polyethylene when the reaction is catalyzed over a metal surface.

Reaction rates are ultimately determined by kinetics, which in the typical formalism will be determined by activation barriers. Towards this end, the energy barriers, with the gas-phase hydrocarbon and the clean platinum slab as the initial state, are shown in Figure 3 (d), along with the adsorption energies for n-alkanes from one to six carbons. A smaller range of n-alkanes was explored in this case for two reasons: (1) the result from the reaction energies suggested that convergence might be achieved at a low number of polyethylene monomers, and (2) it was not possible to guarantee the localization of a genuine transition state for longer chains due to the presence of more than one imaginary frequency in the frequency analysis, even at tight convergence criteria for the forces (0.01 eV $Å^{-1}$) and the energies ($1x10^{-8}$ eV). For pentane and hexane, two imaginary frequencies were observed; however, the second imaginary frequency was significantly smaller than the first one (x cm^{-1} vs y cm^{-1}). Also, the first imaginary frequency

corresponded to the apparent direction of the reaction coordinate, while the second corresponded to a random rotation of the entire molecule. Thus, the second imaginary frequency was disregarded from the analysis. In Figure 3 (d), the energy barriers and the adsorption energies follow the same linear trend and are parallel, as in Figure 3 (a). Therefore, it is expected that the energy *barriers*, calculated by the difference between the linear trends of Figure 3 (d), do not change significantly from one to six carbons, shown graphically in Figure S7 of the Supporting Information. This result implies that once the hydrocarbon is adsorbed to the surface, a methane molecule would exhibit the same activity for the C-H cleavage as a polyethylene molecule.

The results presented up to this point have focused on the C-H cleavage in polyethylene oligomers; we find same trends in the case of the C-C cleavage. Figure 4 (a) shows the RE1s for the C-C cleavage of polyethylene oligomers and the adsorption energies, where the RE1s and adsorption energies exhibit the same linear trend and slope.

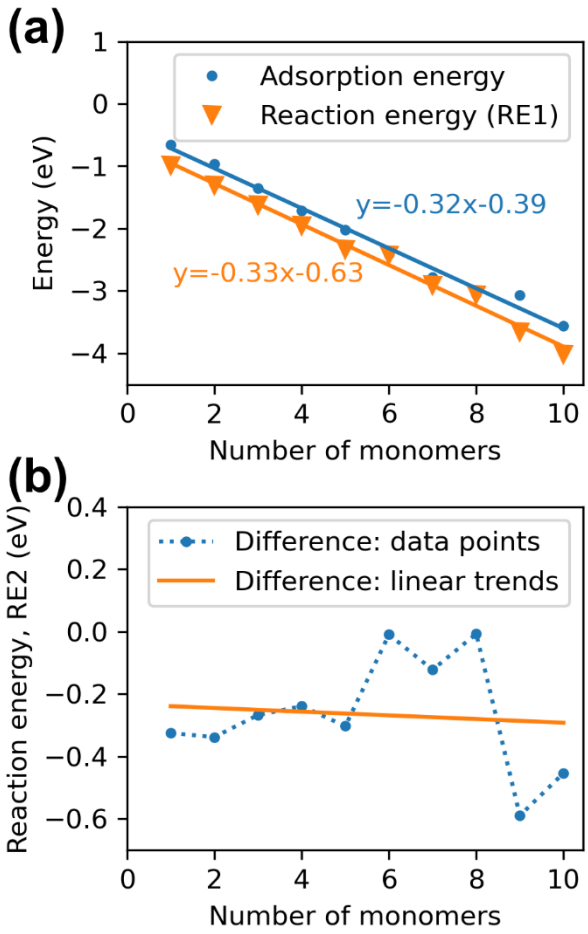

Figure 4. (a) Reaction energies for the C-C cleavage (referred to as RE1 since the initial state is the clean metal slab and gas-phase hydrocarbon) and adsorption energies as a function of the number of monomers in the polyethylene oligomers. (b) Reaction energies for the C-C cleavage (RE2 since the initial state is the adsorbed hydrocarbon) as a function of the number of monomers in the polyethylene oligomers. The RE2s were calculated in two different ways: by the difference between the data points and by the difference between linear trends.

The difference between these linear trends, which represent RE2, is shown in Figure 4 (b), along with the difference between data points. As we hypothesized, the RE2 calculated by the difference between linear trends presented no significant change as the number of monomers increased. Therefore, this result corroborates what was found for the C-H cleavage: an oligomer as small as

ethane could represent the thermodynamics of the C-C cleavage of polyethylene over a metal surface.

On the other hand, the energy barriers could not be determined since finding a transition state for the C-C cleavage of saturated n-alkanes over a metal surface was not possible: the C-C bond always breaks in the gas phase before contacting the metal surface. Probably, the n-alkane has to go through several dehydrogenation steps on the surface before the C-C can be broken, and is supported by the exceptional stability of polyethylene. Still, we expect that the energy barriers would follow the same trend as the adsorption energies, as in the C-H cleavage case.

Finally, the results for the RE1s of C-H and C-C cleavage of PP oligomers are presented in Figure 5. In Figure 5 (a), the RE1s for C-H cleavage and adsorption energies follow the same linear trend and are parallel. These features indicate that the RE2s do not change significantly with the number of monomers (see Figure S8 in the Supporting Information). However, in Figure 5 (b), RE1s for the C-C cleavage follow a linear trend whose slope is slightly different from the slope for the linear trend of the adsorption energies. Qualitatively, this result suggests that the RE2s decrease indefinitely as the number of monomers increases, i.e., the RE2s tend to minus infinity as they approach the size of the full polymer. Most likely, the configurations found for the final state of the C-C cleavage and the adsorbed hydrocarbon are not close to the lowest energy configurations, despite extensive searching via minima hopping. This failure in finding the lowest energy configuration (or a configuration close to it) might be related to the bigger size and more complex structure of polypropylene oligomers compared to polyethylene oligomers, which increases the number of possible configurations over Pt(211) combinatorically and makes it harder to find the ones with the lowest energy. Since the linear trends might change considerably if lower energy configurations are found, and there is no agreement between the C-H and C-C bond

cleavage trends, we find these results to be inconclusive, and a minimum chain length cannot be established from these results to represent the thermodynamics of C-H and C-C cleavage of PP over metal catalysts.

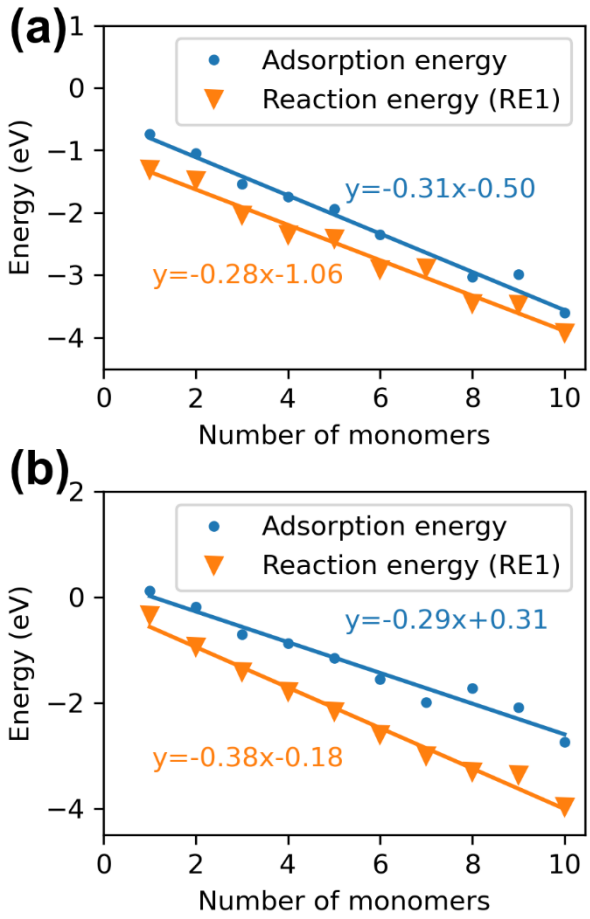

Figure 5. (a) Reaction energies for the C-H cleavage (referred to as RE1 since the initial state is the clean metal slab and gas-phase hydrocarbon) and adsorption energies as a function of the number of monomers in the polypropylene oligomers. (b) RE1s for the C-C cleavage and adsorption energies as a function of the number of monomers in the polypropylene oligomers.

To summarize our findings, we have performed DFT calculations to determine the effect of the number of monomers on the reaction energies and energy barriers of the C-H and C-C cleavage over a metal surface for polyethylene and polypropylene oligomers. Estimates of the global

minimum energy configurations were found using minima hopping and a fine-tuned machine learning model. The fine-tuning of the machine learning model with data from this work decreased the initial MAE of 0.452 eV/atom to 0.0016 eV/atom for the test set, enhancing the accuracy of the energy prediction given an initial structure. We reported a counterintuitive supercell size effect where the system becomes less stable as the surface coverage of the hydrocarbon decreases, in contrast to typically reported adsorbate-adsorbate interactions on metal surfaces. The supercell size effect was compensated for by comparing the different chain lengths using the same supercell size. The reaction energies of C-H and C-C bond cleavage were calculated using two different initial states: (1) the gas phase hydrocarbon and the clean metal slab (RE1) and (2) the adsorbed hydrocarbon over the metal slab (RE2). A linear relationship was observed between the RE1s and the number of monomers for polyethylene and polypropylene oligomers, which was attributed to the vdW interactions. The RE2s for the C-H and C-C cleavage and the energy barriers for the C-H cleavage were not affected by the size of the polyethylene oligomer. Overall, our findings suggest that an oligomer as small as ethane can be used as a model molecule for the degradation and upcycling of polyethylene over metal surfaces. For polypropylene, it was not possible to determine the minimum length of the model molecule since there was a disagreement in the trends for the RE2s of the C-H and C-C bond cleavage. We again wish to highlight that the use of small molecules as a model for polyethylene such as those studied here will necessarily disregard important polymer behaviors such as entanglement and the significant mass transport challenges associated with catalytic polymer upcycling. However, given the significant aforementioned challenges in conducting experiments with polymer systems – in addition to challenges in modeling polymer interactions at metal surfaces with DFT – our findings of simple molecules

being suitable for reproducing critical polymer upcycling energetics will likely be useful in future studies.

COMPUTATIONAL METHODS

Periodic, plane wave density functional theory (DFT) calculations were performed using Vienna ab initio simulation package (VASP),[29,30] interfaced through the Atomic Simulation Environment (ASE).[31] Core electrons of each atom were described with projector augmented wave (PAW) pseudopotentials,[32] and valence electrons were modeled by plane waves up to a kinetic energy cutoff of 500 eV. The revised Perdew-Burke-Ernzerhof (RPBE) functional form of the generalized gradient approximation (GGA)[33] was used to address the exchange-correlation effects, and Grimme's DFT-D3 method[25] with the zero-damping function was used to describe the van der Waals interactions semiempirically. The convergence criterion for the geometry optimizations was when the residual forces were smaller than 0.03 eV $Å^{-1}$. The convergence criterion for the electronic energy in each electronic self-consistency cycle was when the difference between iterations was not more than 10^{-4} eV. The electronic occupancies were determined according to the Gaussian smearing method with a smearing width of 0.05 eV.

Calculations of gas phase species were performed in a 20 x 20 x 40 Å unit cell of vacuum and were computed using a 2 x 2 x 1 Monkhorst-Pack k-point grid. The (211) surface of the fcc metal was selected to carry out the C-H and C-C cleavage due to the higher reactivity of its undercoordinated atoms located at the step.[34] The lattice constant for platinum was optimized without the vdW correction enabled because it has a tendency to substantially reduce the lattice constant. As a result, our surface calculations where the vdW correction is enabled are likely to be 1% strained. Still, this strain did not affect the linear trends observed for the reaction energies (see

Figure S9 of the Supporting Information). The supercell size depended on the type of calculation performed over it (C-H or C-C bond cleavage). Still, all the supercells had three layers of atoms where the first layer was allowed to relax, and the other two layers were constrained to the bulk positions. A vacuum region of 10 Å separated the successive slabs to avoid periodic interactions and a dipole correction was included.[35] For the C-H bond cleavage, a 12x3x3 supercell was used to accommodate the larger hydrocarbon chains along the x-direction. For the C-C bond cleavage, 9x3x3 (polyethylene) and 9x8x3 (polypropylene) supercells were used to fit the segments produced after breaking the C-C bond. In these calculations, the Brillouin zone was sampled with a 32/a x 40/b x 1 Monkhorst -Pack k-point grid, where a and b are the lattice vectors parallel to the XY-plane of the cell.

The transition states were first estimated by constraining the distance between the cleaved hydrogen and the oligomer and calculating the energy at different constrained distances. The highest energy structure was considered the approximate transition state. Then, more accurate transition state structures were obtained using the dimer method as developed and implemented by Henkelman.[36] A force tolerance of 0.01 eV $Å^{-1}$ is used in all the transition state searches. We confirmed localization of a true saddle point by finite difference estimation of the Hessian and identification of a single imaginary vibrational frequency.

The minima hopping global optimization method,[19] implemented through ASE with a temperature of 300 K, was used to find the minimum energy configuration for the structure consisting of the metal slab with the hydrocarbon after the C-H or C-C cleavage. A Hookean constraint with a cutoff distance of 1.59 Å and k = 7 was placed between the C-H and C-C bonds of the n-alkane to prevent undesired spontaneous cleavage of these bonds aside from the bond of interest. The calculator used for this method was the Open Catalyst Project[21] calculator, which is

based on a machine-learning model to determine the energies and forces of the atomic structure. The machine learning model was fine-tuned to the hydrocarbon and metal surface system using the procedure described in the Supporting Information.

ASSOCIATED CONTENT

Supporting Information Available:

- Details for the fine-tuning of the machine learning model. Additional figures showing the effect of omitting the van der Waals interaction in the reaction energy calculation, the reaction energies for the C-H cleavage and adsorption energies as a function of the number of monomers of polyethylene oligomers for different metals, the reaction energies (adsorbed hydrocarbon as the initial state) as a function of the number of monomers in the polypropylene oligomers and a comparison of the reaction energies for the C-H cleavage of polyethylene oligomers with and without vdW correction in the optimization of the bulk metal (PDF).

- Optimized structures, calculation data, and python codes necessary for reproducing all the figures shown in the text. (ZIP file)

Notes

The authors declare no competing financial interests.

ACKNOWLEDGMENT

This research was supported by the US Department of Energy, Office of Science, Office of Basic Energy Sciences, Chemical Upcycling of Polymers Program under Award DE-SC0022307.

REFERENCES

(1) OECD. *Plastic waste by end-of-life fate - projections*. https://www.oecd-ilibrary.org/content/data/3f85b1c2-en.

(2) Bremer, C. *Plastic pollution is growing relentlessly as waste management and recycling fall short, says OECD*. Environment. https://www.oecd.org/en/about/news/press-releases/2022/02/plastic-pollution-is-growing-relentlessly-as-waste-management-and-recycling-fall-short.html (accessed 2024-08-19).

(3) Geyer, R.; Jambeck, J. R.; Law, K. L. Production, Use, and Fate of All Plastics Ever Made. *Sci. Adv.* **2017**, *3* (7), e1700782. https://doi.org/10.1126/sciadv.1700782.

(4) Sun, J.; Dong, J.; Gao, L.; Zhao, Y.-Q.; Moon, H.; Scott, S. L. Catalytic Upcycling of Polyolefins. *Chem. Rev.* **2024**. https://doi.org/10.1021/acs.chemrev.3c00943.

(5) Zou, L.; Xu, R.; Wang, H.; Wang, Z.; Sun, Y.; Li, M. Chemical Recycling of Polyolefins: A Closed-Loop Cycle of Waste to Olefins. *Natl. Sci. Rev.* **2023**, *10* (9), nwad207. https://doi.org/10.1093/nsr/nwad207.

(6) Musa, A.; Jaseer, E. A.; Barman, S.; Garcia, N. Review on Catalytic Depolymerization of Polyolefin Waste by Hydrogenolysis: State-of-the-Art and Outlook. *Energy Fuels* **2024**, *38* (3), 1676–1691. https://doi.org/10.1021/acs.energyfuels.3c04109.

(7) Zhang, W.; Kim, S.; Wahl, L.; Khare, R.; Hale, L.; Hu, J.; Camaioni, D. M.; Gutiérrez, O. Y.; Liu, Y.; Lercher, J. A. Low-Temperature Upcycling of Polyolefins into Liquid Alkanes via Tandem Cracking-Alkylation. *Science* **2023**, *379* (6634), 807–811. https://doi.org/10.1126/science.ade7485.

(8) Ghatge, S.; Yang, Y.; Ahn, J.-H.; Hur, H.-G. Biodegradation of Polyethylene: A Brief Review. *Appl. Biol. Chem.* **2020**, *63* (1), 27. https://doi.org/10.1186/s13765-020-00511-3.

(9) Devi, P.; Soni, A.; Singh, J. P. Highly Effective In2O3-rGO Catalyst for the Photocatalytic Degradation of Polyethylene under Visible Light. *J. Polym. Res.* **2024**, *31* (6), 152. https://doi.org/10.1007/s10965-024-04002-7.

(10) Kim, S.; Kong, D.; Zheng, X.; Park, J. H. Upcycling Plastic Wastes into Value-Added Products via Electrocatalysis and Photoelectrocatalysis. *J. Energy Chem.* **2024**, *91*, 522–541. https://doi.org/10.1016/j.jechem.2024.01.010.

(11) Mais, L.; Melis, N.; Vacca, A.; Mascia, M. Electrochemical Removal of PET and PE Microplastics for Wastewater Treatment. *Environ. Sci. Water Res. Technol.* **2024**, *10* (2), 399–407. https://doi.org/10.1039/D3EW00582H.

(12) Chirinos-Padrón, A. J.; Hernández, P. H.; Chávez, E.; Allen, N. S.; Vasiliou, C.; DePoortere, M. Influences of Unsaturation and Metal Impurities on the Oxidative Degradation of High Density Polyethylene. *Eur. Polym. J.* **1987**, *23* (12), 935–940. https://doi.org/10.1016/0014-3057(87)90036-X.

(13) Rorrer, J. E.; Beckham, G. T.; Román-Leshkov, Y. Conversion of Polyolefin Waste to Liquid Alkanes with Ru-Based Catalysts under Mild Conditions. *JACS Au* **2021**, *1* (1), 8–12. https://doi.org/10.1021/jacsau.0c00041.

(14) Celik, G.; Kennedy, R. M.; Hackler, R. A.; Ferrandon, M.; Tennakoon, A.; Patnaik, S.; LaPointe, A. M.; Ammal, S. C.; Heyden, A.; Perras, F. A.; Pruski, M.; Scott, S. L.; Poeppelmeier,

K. R.; Sadow, A. D.; Delferro, M. Upcycling Single-Use Polyethylene into High-Quality Liquid Products. *ACS Cent. Sci.* **2019**, *5* (11), 1795–1803. https://doi.org/10.1021/acscentsci.9b00722.

(15) Sun, C.; Wang, J.; Wang, J.; Shakouri, M.; Shi, B.; Liu, X.; Guo, Y.; Hu, Y.; Wu, X.-P.; Wang, Y. Pt Enhanced C–H Bond Activation for Efficient and Low-Methane-Selectivity Hydrogenolysis of Polyethylene over Alloyed RuPt/ZrO2. *Appl. Catal. B Environ. Energy* **2024**, *353*, 124046. https://doi.org/10.1016/j.apcatb.2024.124046.

(16) Yuan, Y.; Xie, Z.; Turaczy, K. K.; Hwang, S.; Zhou, J.; Chen, J. G. Controlling Product Distribution of Polyethylene Hydrogenolysis Using Bimetallic RuM3 (M = Fe, Co, Ni) Catalysts. *Chem Bio Eng.* **2024**, *1* (1), 67–75. https://doi.org/10.1021/cbe.3c00007.

(17) Knyazev, V. D. Effects of Chain Length on the Rates of C−C Bond Dissociation in Linear Alkanes and Polyethylene. *J. Phys. Chem. A* **2007**, *111* (19), 3875–3883. https://doi.org/10.1021/jp066419e.

(18) Alkorta, I.; Elguero, J. The Carbon–Carbon Bond Dissociation Energy as a Function of the Chain Length. *Chem. Phys. Lett.* **2006**, *425* (4), 221–224. https://doi.org/10.1016/j.cplett.2006.05.050.

(19) Goedecker, S. Minima Hopping: An Efficient Search Method for the Global Minimum of the Potential Energy Surface of Complex Molecular Systems. *J. Chem. Phys.* **2004**, *120* (21), 9911–9917. https://doi.org/10.1063/1.1724816.

(20) Meta AI; Carnegie Mellow University. *Open Catalyst Project*. https://opencatalystproject.org/.

(21) Zitnick, C. L.; Chanussot, L.; Das, A.; Goyal, S.; Heras-Domingo, J.; Ho, C.; Hu, W.; Lavril, T.; Palizhati, A.; Riviere, M.; Shuaibi, M.; Sriram, A.; Tran, K.; Wood, B.; Yoon, J.; Parikh, D.; Ulissi, Z. An Introduction to Electrocatalyst Design Using Machine Learning for Renewable Energy Storage. arXiv October 14, 2020. https://doi.org/10.48550/arXiv.2010.09435.

(22) Chanussot, L.; Das, A.; Goyal, S.; Lavril, T.; Shuaibi, M.; Riviere, M.; Tran, K.; Heras-Domingo, J.; Ho, C.; Hu, W.; Palizhati, A.; Sriram, A.; Wood, B.; Yoon, J.; Parikh, D.; Zitnick, C. L.; Ulissi, Z. Open Catalyst 2020 (OC20) Dataset and Community Challenges. *ACS Catal.* **2021**, *11* (10), 6059–6072. https://doi.org/10.1021/acscatal.0c04525.

(23) Tran, R.; Lan, J.; Shuaibi, M.; Wood, B. M.; Goyal, S.; Das, A.; Heras-Domingo, J.; Kolluru, A.; Rizvi, A.; Shoghi, N.; Sriram, A.; Therrien, F.; Abed, J.; Voznyy, O.; Sargent, E. H.; Ulissi, Z.; Zitnick, C. L. The Open Catalyst 2022 (OC22) Dataset and Challenges for Oxide Electrocatalysts. *ACS Catal.* **2023**, *13* (5), 3066–3084. https://doi.org/10.1021/acscatal.2c05426.

(24) Musielewicz, J.; Wang, X.; Tian, T.; Ulissi, Z. FINETUNA: Fine-Tuning Accelerated Molecular Simulations. *Mach. Learn. Sci. Technol.* **2022**, *3* (3), 03LT01. https://doi.org/10.1088/2632-2153/ac8fe0.

(25) Grimme, S.; Antony, J.; Ehrlich, S.; Krieg, H. A Consistent and Accurate Ab Initio Parametrization of Density Functional Dispersion Correction (DFT-D) for the 94 Elements H-Pu. *J. Chem. Phys.* **2010**, *132* (15), 154104. https://doi.org/10.1063/1.3382344.

(26) Sexton, B. A.; Hughes, A. E. A Comparison of Weak Molecular Adsorption of Organic Molecules on Clean Copper and Platinum Surfaces. *Surf. Sci.* **1984**, *140* (1), 227–248. https://doi.org/10.1016/0039-6028(84)90394-7.

(27) Tait, S. L.; Dohnálek, Z.; Campbell, C. T.; Kay, B. D. N-Alkanes on Pt(111) and on C(0001)/Pt(111): Chain Length Dependence of Kinetic Desorption Parameters. *J. Chem. Phys.* **2006**, *125* (23), 234308. https://doi.org/10.1063/1.2400235.

(28) Ding, X.; Zhu, H.; Ren, H.; Liu, D.; Yu, Z.; Shi, N.; Guo, W. Adsorption and Dehydrogenation of C 2 –C 6 n -Alkanes over a Pt Catalyst: A Theoretical Study on the Size Effects of Alkane Molecules and Pt Substrates. *Phys. Chem. Chem. Phys.* **2020**, *22* (38), 21835–21843. https://doi.org/10.1039/D0CP03194A.

(29) Kresse, G.; Furthmüller, J. Efficient Iterative Schemes for Ab Initio Total-Energy Calculations Using a Plane-Wave Basis Set. *Phys. Rev. B* **1996**, *54* (16), 11169–11186. https://doi.org/10.1103/PhysRevB.54.11169.

(30) Kresse, G.; Furthmüller, J. Efficiency of Ab-Initio Total Energy Calculations for Metals and Semiconductors Using a Plane-Wave Basis Set. *Comput. Mater. Sci.* **1996**, *6* (1), 15–50. https://doi.org/10.1016/0927-0256(96)00008-0.

(31) Bahn, S. R.; Jacobsen, K. W. An Object-Oriented Scripting Interface to a Legacy Electronic Structure Code. *Comput. Sci. Eng.* **2002**, *4* (3), 56–66. https://doi.org/10.1109/5992.998641.

(32) Kresse, G.; Joubert, D. From Ultrasoft Pseudopotentials to the Projector Augmented-Wave Method. *Phys. Rev. B* **1999**, *59* (3), 1758–1775. https://doi.org/10.1103/PhysRevB.59.1758.

(33) Hammer, B.; Hansen, L. B.; Nørskov, J. K. Improved Adsorption Energetics within Density-Functional Theory Using Revised Perdew-Burke-Ernzerhof Functionals. *Phys. Rev. B* **1999**, *59* (11), 7413–7421. https://doi.org/10.1103/PhysRevB.59.7413.

(34) Liu, Z.-P.; Hu, P. General Rules for Predicting Where a Catalytic Reaction Should Occur on Metal Surfaces: A Density Functional Theory Study of C−H and C−O Bond Breaking/Making on Flat, Stepped, and Kinked Metal Surfaces. *J. Am. Chem. Soc.* **2003**, *125* (7), 1958–1967. https://doi.org/10.1021/ja0207551.

(35) Bengtsson, L. Dipole Correction for Surface Supercell Calculations. *Phys. Rev. B* **1999**, *59* (19), 12301–12304. https://doi.org/10.1103/PhysRevB.59.12301.

(36) Heyden, A.; Bell, A. T.; Keil, F. J. Efficient Methods for Finding Transition States in Chemical Reactions: Comparison of Improved Dimer Method and Partitioned Rational Function Optimization Method. *J. Chem. Phys.* **2005**, *123* (22), 224101. https://doi.org/10.1063/1.2104507.